

MCT4 regulates de novo pyrimidine biosynthesis in GBM in a lactate-independent manner

Raffaella Spina, Dillon M. Voss, Xiaohua Yang, Jason W. Sohn, Robert Vinkler, Julianna Schraner, Anthony Sloan, Scott M. Welford, Norbert Avril, Heather M. Ames, Graeme F. Woodworth, and Eli E. Bar[®]

Department of Pathology, University of Maryland School of Medicine, Baltimore, Maryland, USA (R.S., H.M.A., E.E.B.); Department of Neurosurgery, University of Maryland School of Medicine, Baltimore, Maryland, USA (R.S., G.F.W., E.E.B.); Marlene and Stewart Greenebaum Comprehensive Cancer Center, University of Maryland School of Medicine, Baltimore, Maryland, USA (R.S., H.M.A., G.F.W., E.E.B.); Department of Neurological Surgery, Case Western Reserve University School of Medicine, Cleveland, Ohio, USA (D.M.V., A.S.); Department of Radiation Oncology, Case Western Reserve University School of Medicine, Cleveland, Ohio, USA (X.Y., J.W.S., R.V., J.S.); Department of Radiology, Division of Nuclear Medicine, Case Western Reserve University School of Medicine, Cleveland, Ohio, USA (N.A.); Department of Radiation Oncology, Miller School of Medicine, University of Miami, Miami, Florida, USA (S.M.W.); Sylvester Comprehensive Cancer Center, Miller School of Medicine, University of Miami, Miami, Florida, USA (S.M.W.)

Corresponding Author: Eli E. Bar, PhD, Departments of Pathology and Neurosurgery, Marlene and Stewart Greenebaum Comprehensive Cancer Center, University of Maryland School of Medicine, 655 W. Baltimore St., Bressler Research Bldg, Room 8-039, Baltimore, MD 21201, USA (ebar@som.umaryland.edu).

Abstract

Background. Necrotic foci with surrounding hypoxic cellular pseudopalisades and microvascular hyperplasia are histological features found in glioblastoma (GBM). We have previously shown that monocarboxylate transporter 4 (MCT4) is highly expressed in necrotic/hypoxic regions in GBM and that increased levels of MCT4 are associated with worse clinical outcomes.

Methods. A combined transcriptomics and metabolomics analysis was performed to study the effects of MCT4 depletion in hypoxic GBM neurospheres. Stable and inducible MCT4-depletion systems were used to evaluate the effects of and underlying mechanisms associated with MCT4 depletion in vitro and in vivo, alone and in combination with radiation.

Results. This study establishes that conditional depletion of MCT4 profoundly impairs self-renewal and reduces the frequency and tumorigenicity of aggressive, therapy-resistant, glioblastoma stem cells. Mechanistically, we observed that MCT4 depletion induces anaplerotic glutaminolysis and abrogates de novo pyrimidine biosynthesis. The latter results in a dramatic increase in DNA damage and apoptotic cell death, phenotypes that were readily rescued by pyrimidine nucleosides supplementation. Consequently, we found that MCT4 depletion promoted a significant prolongation of survival of animals bearing established orthotopic xenografts, an effect that was extended by adjuvant treatment with focused radiation.

Conclusions. Our findings establish a novel role for MCT4 as a critical regulator of cellular deoxyribonucleotide levels and provide a new therapeutic direction related to MCT4 depletion in GBM.

Key Points

- MCT4 Depletion in Brain Cancer—Associated *Hypoxia*
- Inhibits *de novo* pyrimidine biosynthesis—leading to the accumulation of DNA damage and reduced cell survival.
- Further extends the survival of animals bearing orthotopic GBM xenografts and treated with focused radiation.

Importance of the Study

GBM is an aggressive, lethal, and still incurable malignancy. Treatment for GBM has changed little in decades. Using a combined metabolomics and transcriptomics approach, we show that MCT4 depletion significantly reduces tumorigenicity by inhibition of de novo

pyrimidine biosynthesis and promotes accumulation of DNA damage. The combination of MCT4 depletion and adjuvant radiation *in vivo* is more effective than either treatment alone thus highlighting the potential for a novel GBM treatment strategy.

Glioblastoma (GBM) is the most common form of malignant brain cancer in adults and remains universally lethal. Despite standard of care therapy that involves maximal surgical resection followed by radiation and temozolomide chemotherapy median survival remains dismal with most patients succumbing to the disease within 2 years of diagnosis.^{1,2} Accumulating evidence suggests that treatment failure and the inevitable recurrence of GBM after therapy are primarily due to the persistence of subpopulations of chemo- and radio-resistant cells, often referred to as glioma stem cells (GSCs).³ Thus, new therapeutic targets and improved treatments that eliminate GSCs and can be combined with the current standard of care are desperately needed. GBM frequently exhibits tumor hypoxia and high glycolytic rate.⁴ We and others have previously shown that GSCs favor low oxygen levels and are typically found in the hypoxic tumor core^{5–10} (and reviewed in Refs 11,12). In addition to hypoxia, GBM is also characterized by a high proliferative index and replication stress contributes to aberrant constitutive activation of DNA damage signaling whereas the inability to repair DNA damage leads to apoptosis.^{13,14}

More recently, we demonstrated that monocarboxylate transporter 4 (MCT4) expression is associated with increased World Health Organization glioma grade and inversely correlated with the overall survival of patients. In addition, MCT4 regulates proliferation, survival, and xenograft implantation.¹⁵ In the current study, we further explore the mechanistic underpinning of MCT4 depletion and its potential utilization in combination with radiation treatment.

Materials and Methods

An expanded Materials and Methods section is provided in Supplementary data.

GBM Neurosphere Lines and Hypoxic Conditions

HSR-GBM1 and HSR040821 were a kind gift from Dr. Angelo Vescevi and were established from freshly resected GBM tumors and passaged as previously described.³ A hypoxic chamber maintained at 37°C, 1% O₂, 5% CO₂, and 94% N₂ (Coy Laboratory Equipment) was used to conduct *in vitro* hypoxic experiments. Because the expression of MCT4 is largely dependent on hypoxia, unless otherwise noted, we used hypoxic culture conditions in all experiments. All hypoxic experiments were conducted on cells

that were plated and allowed to recover overnight before hypoxic induction.

HSR-GBM1 and HSR040821 are EGFR^{WT}, IDH1^{WT}. HSR-GBM1 is P53^{WT} while HSR040821 carries an S278P point mutation in the P53 gene. The Phosphatase and Tensin homolog gene is intact in both lines.

Metabolomics

Focused (quantitative) metabolomics was performed on hypoxic GBM neurospheres with or without MCT4 depletion. Samples were processed and analyzed by the University of Michigan Medical School, BRCF—Metabolomics Core.

Gene Set Enrichment Analysis

Gene set enrichment analysis (GSEA) was performed according to¹⁶ RNA sequencing data, performed in triplicates, of hypoxic and normoxic HSR-GBM1 neurospheres expressing control or shMCT4 were uploaded to the GSEA portal and gene sets enriched in hypoxic GSCs and in hypoxic GSCs depleted of MCT4 were determined.

Glutamine Uptake Assays

Cells were incubated in glucose/glutamine-free media supplemented with 1 μCi/ml [C-14]deoxyglucose (DG) and 1 μCi/ml [H-3]glutamine (GLN), then washed, and added to tubes containing scintillation fluid. Radioactivity was measured and is expressed as pmoles uptake of tracer per 10 000 live cells. Experiments were performed 3 times in duplicates.

Cellular Growth and Clonogenic Assays

Clonogenic assays were performed as previously described.⁶

Immunofluorescence

Cells were cultured in multi-chamber slides and treated as described. Cells were immunostained with α-phospho (ser139)-H2AX antibodies. Nuclei were counterstained with 4',6-diamidino-2-phenylindole. The number of γH2AX-positive foci per cell was counted, using ImageJ.

Alkaline Comet assay

Comet assays were performed as previously described.¹⁷

Flow Cytometry

Mitochondrial membrane potential was evaluated utilizing MitoTracker Red CMXRos according to the manufacturer's instructions.

Orthotopic Xenograft Transplantation

Experiments with animals were performed in compliance with institutional guidelines and regulations (IACUC #2012–0132 followed by #2015–0100). Male and female NSG mice were used in all experiments in approximately equal numbers (± 1) of each sex in each experimental group. Cells were stereotactically injected as previously described.¹⁸ Two separate in vivo experiments were performed using a total of 16 mice per group: control, radiation (IR, 12 Gy), doxycycline (for MCT4 knockdown), and doxycycline combined with IR. Also, to exclude pharmacologic toxicity of doxycycline, HSR-GBM1-shGFP Luciferase cells were implanted into mice using a total of 6 mice per group. Mice weight was monitored daily. Doxycycline was provided in the food at a concentration of 200 mg/kg (#S3888, BioServ), supplied fresh every week starting 3 days before radiation treatment.

Gamma Knife Radiation

Isocentric gamma radiation dose delivery (Gamma Knife) was performed using a three-dimensional (3D)-printed stereotactic body mold as described in Ref. 19.

Statistical Methods

Statistical methods are described throughout the text and summarized in the expanded Materials and Methods section found in the Supplementary data.

Results

MCT4 Knockdown Inhibits GSC Growth and Self-Renewal In Vitro

To investigate the requirement for hypoxia-induced MCT4 for GSC proliferation and/or survival, we conducted in vitro proliferation and self-renewal assays on a set of human GSC lines using either control or 2 different MCT4 short hairpin RNAs (shRNAs). MCT4 depletion significantly impaired growth by at least 40% in both HSR-GBM1 and HSR040821 (Figure 1A and B). To determine the effect of MCT4 depletion on self-renewal, neurospheres expressing control or 2 different MCT4 shRNAs were cultured in hypoxia for 48 h followed by self-renewal challenge in normoxia.⁶ MCT4 depletion resulted in a 60–90% (**** $P < .0001$, one-way ANOVA) and 80–83% reduction (**** $P < .0001$, *** $P < .001$, one-way ANOVA) in the number of

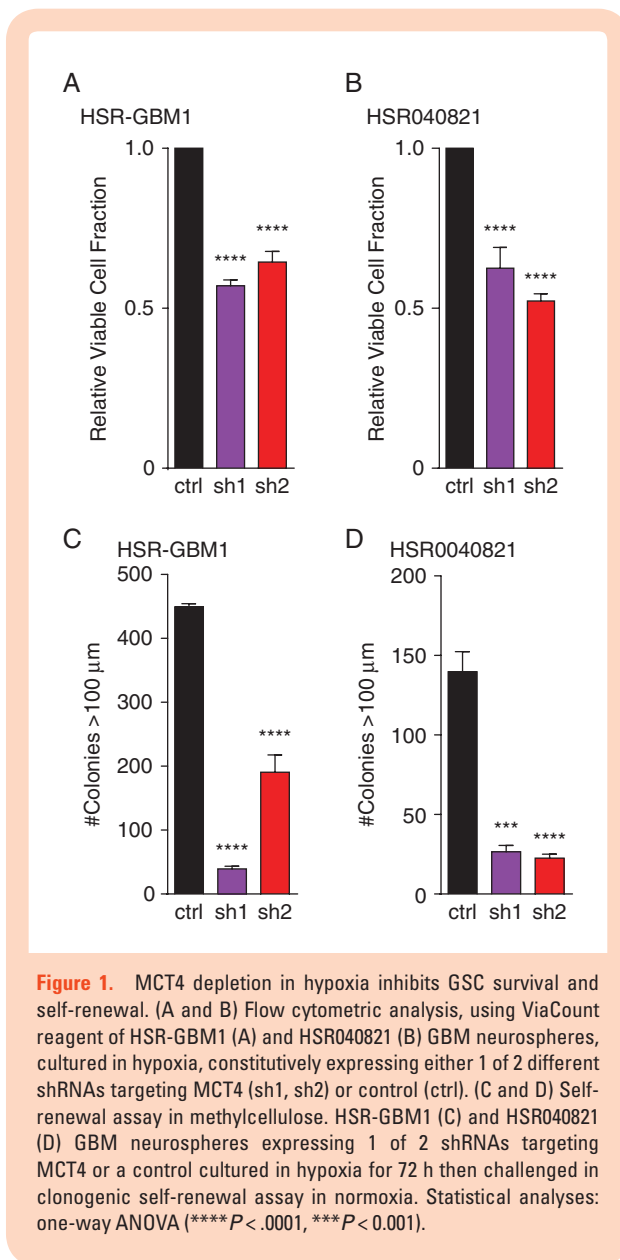
clonogenic neurospheres (sphere diameter $>100 \mu\text{m}$), in HSR-GBM1 and HSR040821, respectively (Figure 1C and D).

GSEA Shows Activation of Metabolic and DNA Repair Pathways in Response to MCT4 Depletion

To identify pathways altered in MCT4-depleted GSCs, we applied GSEA, using cancer hallmarks gene sets, to RNAseq data generated from HSR-GBM1 shMCT4Tet-ON cultured in hypoxia and induced with doxycycline or vehicle as control (Supplementary Figure S1). As expected, the top gene sets, enriched in hypoxic GSCs (top panel of Figure 2, control), included hypoxia and glycolysis (Figure 2A and B). In addition, and in agreement with previous reports, mammalian target of rapamycin complex 1 (MTORC1)²⁰ and the unfolded protein response²¹ were also enriched in hypoxic GSCs (Figure 2C and D). In contrast, MCT4-depleted GSCs showed enrichment for the oxidative phosphorylation (OXPHOS), mitotic spindle, DNA repair, and G2/M checkpoint (lower panel, Figure 2E and H) gene sets, where the last 3 are indicative of potential accumulation of DNA damage.

Depletion of MCT4, in Hypoxia, Inhibits Glycolysis and Increases TCA Cycle Intermediates and Aspartate Through Mitochondria Reactivation

To better understand the metabolic changes MCT4-depleted cells undergo, we conditionally depleted MCT4 in HSR-GBM1 neurospheres cultured in hypoxia (1% oxygen) followed by targeted (quantitative) metabolomics analysis of over 150 metabolites involved in several key metabolic pathways. We found that the levels of 11 out of 18 amino acids measured to be modestly reduced in MCT4-depleted cells (Figure 3A). In contrast, glutamine and aspartate levels were both increased over 2-fold. Glycolysis was inhibited as well as we documented a significant reduction in the levels of several glycolytic intermediates such as dihydroxyacetone phosphate (DHAP), 3-phosphoglycerate, and 2-phosphoglycerate. Glycerol-3-phosphate, which is synthesized by reducing DHAP by the enzyme glycerol-3-phosphate dehydrogenase, was also significantly reduced (Figure 3B). Consistent with our previous reports, lactate levels were not significantly altered in MCT4-depleted neurospheres.^{15,22} In contrast, we found that the levels of The citric acid (TCA) cycle intermediates citrate/isocitrate, α -ketoglutarate, and malate all significantly increased in MCT4-depleted, hypoxic neurospheres (Figure 3C). The significant increase in aspartate levels suggested that mitochondria may be activated,²³ albeit under conditions known to shut mitochondria off. To test this directly, we stained HSR040821 neurospheres with the cell-permeant MitoTracker Red CMXRos that accumulates and fluoresces in active mitochondria and analyzed cells by flow cytometry. Indeed, we found a 3.5-fold increase in the percentage of MitoTracker-positive cells in hypoxic, MCT4-depleted, neurospheres as compared to controls (Figure 3E). Finally, the increase in glutamine levels prompted us to determine if it may be the result of increased uptake as a potential adaptation to reduced glycolysis. To this end, we performed



radioactive tracer uptake experiments to directly measure the uptake of radioactive glutamine in HSR-GBM1 shMCT4 Tet-ON neurospheres cultured in hypoxia and either depleted of MCT4 (dox) or not (v). In these experiments, we documented a moderate but very significant increase in H-3-glutamine uptake in MCT4-depleted cells confirming that the increase in cellular glutamine levels is likely the result of increased glutamine uptake from the medium (Figure 3F).

MCT4 Depletion in Hypoxia Attenuates Nucleotide Biosynthesis and Leads to Accumulation of DNA Damage

The most significant metabolic alterations in hypoxic MCT4-depleted neurospheres were in nucleotides and their precursors (Figure 3D). It has been previously shown

that alterations in nucleotide availability can promote mitotic catastrophe and induce DNA damage.²⁴ Considering our GSEAs showing enrichment for DNA damage pathways, we hypothesized that MCT4 depletion, in hypoxia, induces DNA damage due to alterations in nucleotide availability. We first analyzed mRNA levels of all 57 genes of the de novo pyrimidine metabolic pathway (from KEGG) and found 15 to be significantly downregulated in MCT4-depleted neurospheres. The expression of dihydroorotate dehydrogenase (DHODH), the rate-limiting enzyme in the pathway, was reduced by almost 30% and the expression of CAD (carbamoyl-phosphate synthetase 2, aspartate transcarbamylase, and dihydroorotase), a trifunctional protein that is associated with the enzymatic activities of the first 3 enzymes in the pathway, was reduced almost 50% (Figure 4A). Importantly, the expression of DHODH and CAD each is significantly higher in GBM as compared to controls (TCGA) and is associated with poor outcome (REMBRANDT; Supplementary Figure S2A–D). We confirmed the reduction in DHODH and CAD by qPCR (Supplementary Figure S2E and F) and of DHODH by Western blot (Supplementary Figure S2G) analyses in MCT4-depleted hypoxic HSR-GBM1 and HSR040821 neurospheres. Western blot analyses for CAD protein were inconsistent, in some experiments confirming reduction and in other showing similar levels in MCT4-depleted and control hypoxic GSCs (not shown). To directly visualize and quantify DNA damage, we performed immunostaining against γ H2AX, a common marker used to label double-strand breaks (DSBs) in DNA, in hypoxic neurospheres where MCT4 expression was inhibited either conditionally or constitutively. qPCR analysis confirmed MCT4 knockdown and Western blot analyses showed a large increase in the amount of phosphorylated H2AX (γ H2AX) (Supplementary Figure S3A and B). At the cellular level, we found a large increase in the number of γ H2AX-positive nuclei in hypoxic, MCT4-depleted, neurospheres (Figure 4B). Quantification of 2 independent experiments is shown in Figure 4D, with HSR-GBM1 showing an averaged increase from 24% to 54.7% and 45.5% (constitutive sh1 and sh2, respectively; *** $P < .001$, * $P < .05$ one-way ANOVA), HSR040821 showing an averaged increase from 9.8% to 31% and 67% (sh1 and sh2, respectively; *** $P < .001$, **** $P < .0001$ one-way ANOVA), and HSR-GBM1 shMCT4 Tet-ON showing an averaged increase from 18% to 46% (**** $P < .0001$ student *t* test).

The alkaline comet assay is a sensitive method that allows detection and quantification of the extent of DNA damage.^{25,26} Comet tail length was measured as it is a widely accepted parameter reporting on the presence of single-strand breaks and DSBs. Representative comets are shown in Figure 4C and the quantification of 2 independent experiments is shown in Figure 4E. These experiments revealed that the number of cells with comet tails increased more rapidly in MCT4-depleted neurospheres as compared to controls. Tail length increased in HSR-GBM1 26.6-fold and 13.8-fold (constitutive sh1 and sh2, respectively; *** $P < .001$ one-way ANOVA) and 16.8-fold and 17.6-fold in HSR040821 expressing sh1 and sh2 constitutively (one-way ANOVA **** $P < .0001$). Similarly, in MCT4-depleted HSR-GBM1 shMCT4 Tet-ON cells, induced to express sh1 with doxycycline, we documented

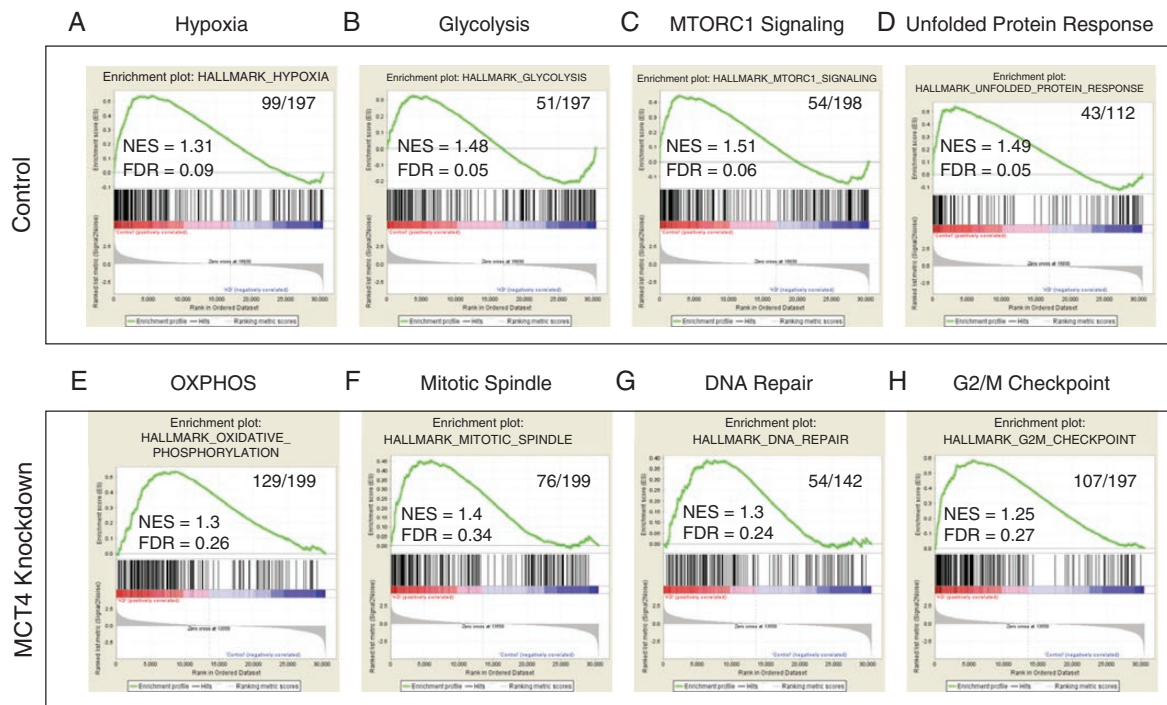


Figure 2. Gene set enrichment analysis. Gene sets of hypoxia (A), glycolysis (B), MTORC1 (C), and unfolded protein response to cellular stress (D) are enriched in HSR-GBM1 shMCT4 Tet-ON (sh1) uninduced (control) neurospheres cultured in hypoxia (1% oxygen) and normoxia. Conditional, doxycycline-induced, knockdown of MCT4, in hypoxia, promotes a complete metabolic signature shift toward oxidative phosphorylation (E) and enriches for pathways indicative of potential DNA damage: mitotic spindle (F), DNA repair (G), and G2/M checkpoint (H). NES, normalized enrichment score; FDR, false discovery rate.

a 4.9-fold increase in comet tail length (t test $***P < .001$). Finally, MCT4 depletion showed negligible effects on tail length and γ H2AX in HSR-GBM1 or HSR040821 cells cultured in normoxia (Supplementary Figure S3C–G). To test if hypoxic depletion of MCT4 promotes DNA damage by perturbing nucleotide pools, we supplemented the growth medium of control and MCT4-depleted neurospheres with nucleosides in an attempt to rescue the effects of MCT4 depletion on cell viability and DNA damage. Here, we documented 43% and 46% reduction in viable cell fractions in HSR-GBM1 neurospheres expressing sh1 and sh2, respectively (one-way ANOVA $*P < .05$ and $**P < .01$, respectively) (Figure 5A). Similarly, in HSR040821, sh1 and sh2 reduced the viable cell fraction by 56% and 48% (one-way ANOVA $***P < .001$) (Figure 5B). Importantly, in both lines supplementation with nucleosides largely blocked these effects (Figure 5A and B). Finally, similar results were obtained with conditional depletion of MCT4 leading to 27% reduction in the viable cell fraction in HSR-GBM1 shMCT4 Tet-ON cells treated with doxycycline (Figure 5C). Because pyrimidines were the most affected by MCT4 depletion, we also tested if supplementation with either one of the pyrimidine nucleosides, cytidine or uridine, would be sufficient to rescue the effects of MCT4 inhibition. As shown in Figure 5C, each cytidine or uridine was sufficient to block the effects of MCT4 depletion. These data suggest

that MCT4 depletion promotes GSC death primarily by reducing pyrimidine nucleotide pools.

To test the effects of nucleoside supplementation on DNA damage, we cultured GBM neurospheres expressing control or 1 of 2 shMCT4 constructs for 48 h in hypoxia in medium supplemented, or not, with nucleosides. In HSR-GBM1, MCT4 depletion increased γ H2AX-positive nuclei from 24% to 54.8% and 45.5% (sh1 and sh2, respectively; $*P < .05$, $***P < .001$, $****P < .0001$, one-way ANOVA; Figure 5D). In HSR040821 MCT4 depletion increased γ H2AX-positive nuclei from 18.8% to 36.5% and 59.1% (sh1 and sh2, respectively; $*P < .05$, $***P < .001$, $****P < .0001$, one-way ANOVA; Figure 5E). Finally, similar results were obtained with conditional MCT4 depletion in HSR-GBM1 shMCT4 Tet-ON, increasing γ H2AX-positive nuclei from 15.8% to 35.7% ($****P < .0001$, one-way ANOVA), and supplementation with either cytidine or uridine pyrimidine nucleosides completely blocked the accumulation of nuclear γ H2AX foci following MCT4 depletion (Figure 5F).

Leflunomide, a Specific Inhibitor of DHODH Mimics the Effects of MCT4 Depletion

If the antitumor effect of MCT4 depletion is strictly dependent on shutting down pyrimidine synthesis, then these effects should be comparable to pharmacological

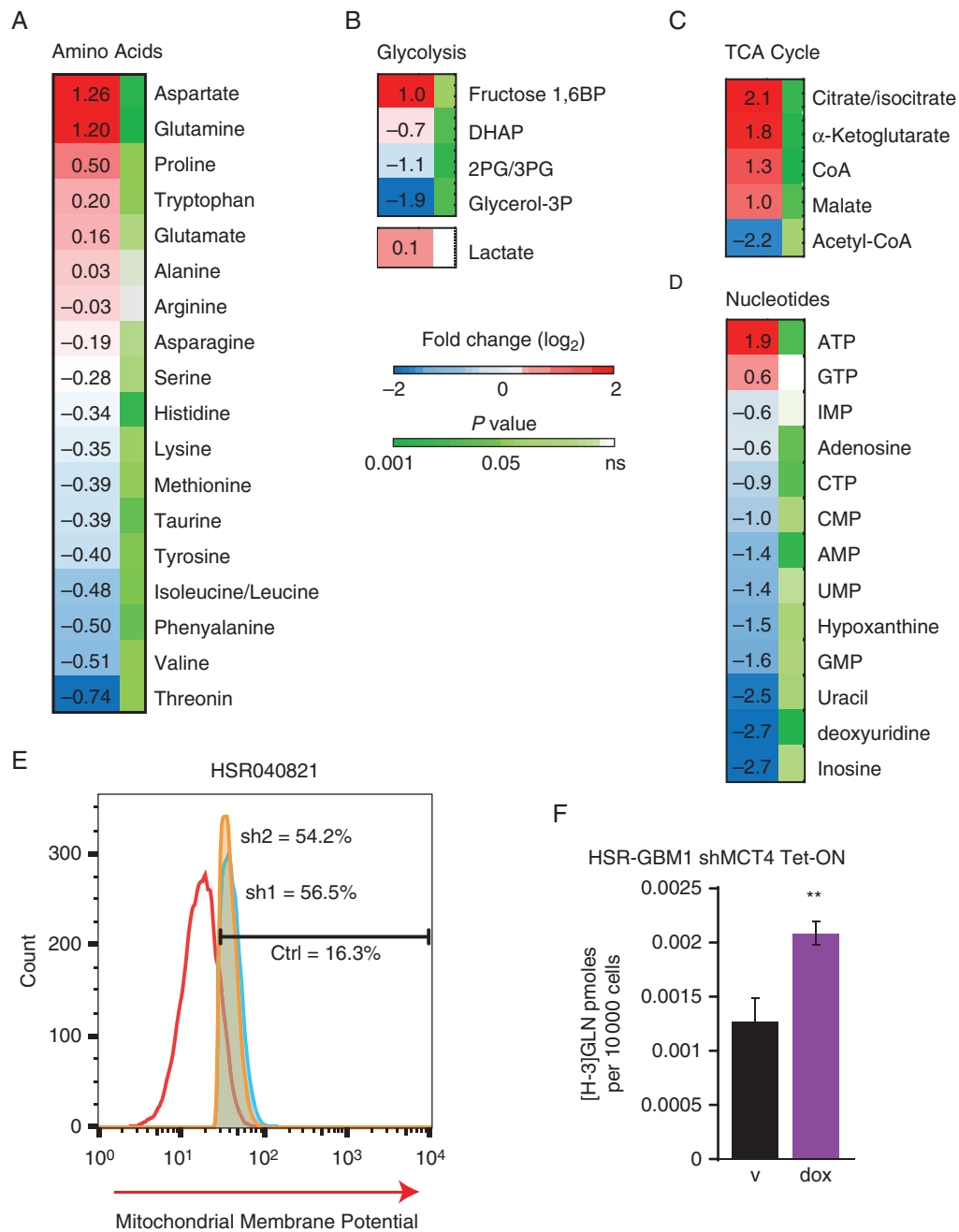


Figure 3. MCT4 depletion promotes metabolic reprogramming in hypoxic GBM neurospheres. Targeted metabolomics analysis of amino acid (A) glycolysis (B), TCA cycle (C), and nucleotide biomolecules (D) in HSR-GBM1 shMCT4 Tet-ON cells cultured in hypoxia and treated with vehicle or 750 nM doxycycline (dox). The heatmap depicts relevant metabolites that were detected as fold change (\log_2) in MCT4-depleted versus non-depleted cells. Data are shown as mean values of replicates. *P* values were derived by a two-sided *t* test; ns, not significant. (E) Flow cytometric analysis of mitochondrial membrane potential in control (Ctrl) and MCT4-depleted (sh1, sh2) HSR040821 using MitoTracker Red CMXRos. The histogram shows representative flow cytometric analysis ($n = 3$). (F) [H-3] Glutamine uptake in hypoxic HSR-GBM1 shMCT4 Tet-ON cells treated with vehicle or doxycycline. The bar graph shows the average of 3 experiments each performed in duplicates. Statistics used: *t* test $**P < .01$.

inhibition of this pathway by the FDA-approved DHODH inhibitor Leflunomide. To test this, we cultured HSR-GBM1 and HSR040821 neurospheres in hypoxia and then treated the cells with Leflunomide for 24 h. We then

measured the effects of Leflunomide on GSC survival and DNA damage. We found that like MCT4 depletion, Leflunomide inhibited GSC growth. Leflunomide treatment reduced the fraction of viable cells by approximately

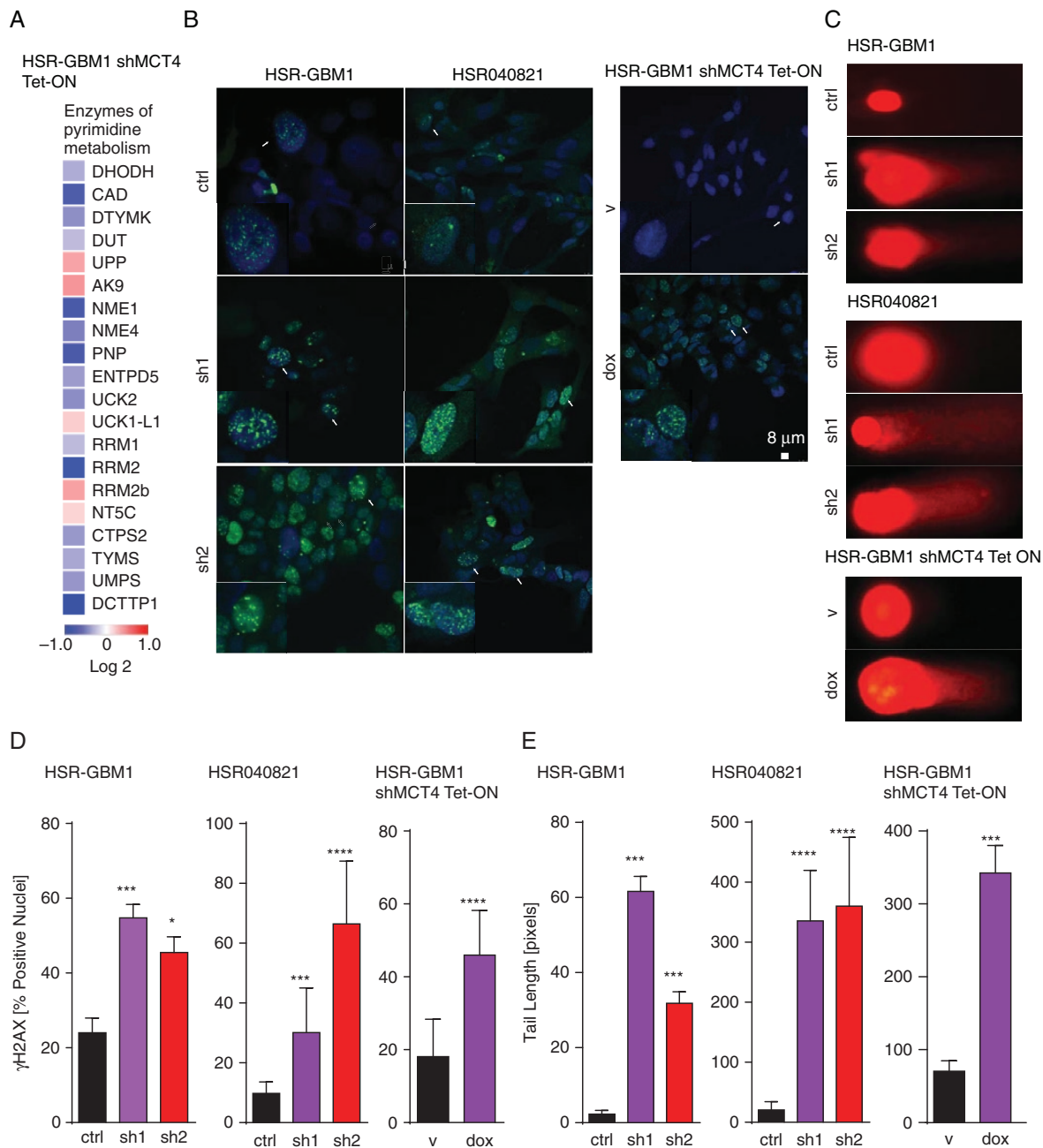


Figure 4. MCT4 depletion inhibits the expression of key pyrimidine biosynthesis enzymes leading to the accumulation of DNA damage in hypoxia. HSR-GBM1 and HSR040821 integrate control (ctrl) or 1 of 2 constitutive shMCT4 constructs (sh1, sh2). HSR-GBM1 neurospheres integrating a conditional shMCT4 Tet-ON were treated with vehicle (v) or doxycycline (dox) to induce shRNA expression. (A) Differential expression levels of 15, KEGG-defined pyrimidine metabolism enzymes (RNAseq, log₂ transformed). (B) Immunocytochemical staining for γ H2AX foci in control and MCT4-depleted neurospheres cultured in hypoxia. (C) Alkaline comet assays performed on GBM neurosphere cells depleted of MCT4 constitutively or conditionally. (D and E) Quantification of the data shown in B and C, respectively (average of 2 independent experiments each). Statistics used: *t* test and one-way ANOVA ****P* < .001, *****P* < .0001. Scale bar represents 8 μ m.

90% and 30%, in HSR-GBM1 and HSR040821, respectively (Figure 5G). These effects are likely due to an increase in DNA damage as we documented a 21-fold and 18-fold increase in γ H2AX-positive nuclei in

HSR-GBM1 and HSR040821, respectively (Figure 5H). Taken together, these results strongly suggest that MCT4 and Leflunomide inhibit a common pathway, namely, de novo pyrimidine synthesis.

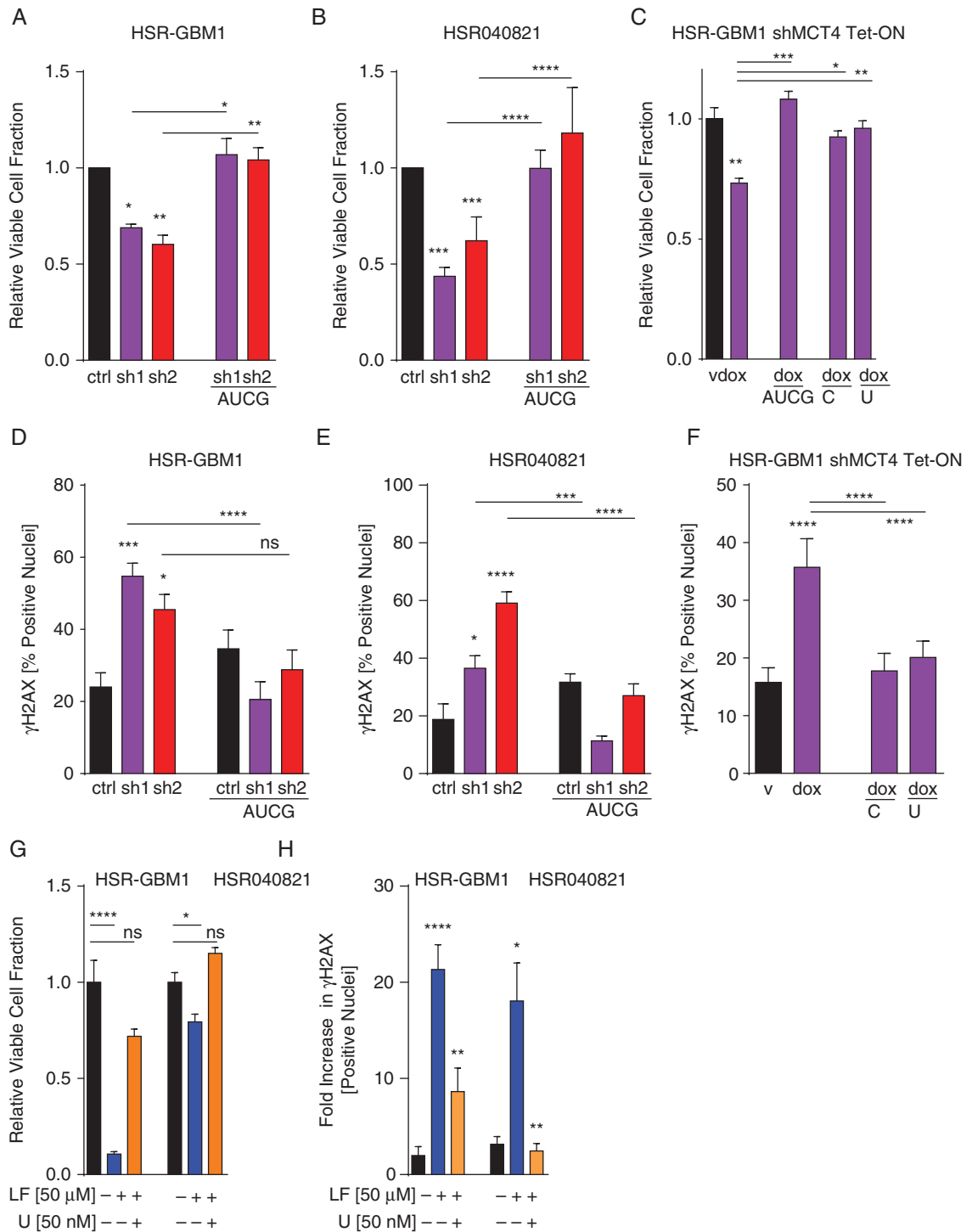


Figure 5. Nucleosides supplementation rescues the effects of MCT4 depletion on growth and DNA damage. Relative viable cell fractions of HSR-GBM1 (A) and HSR040821 (B), expressing control or 1 of 2 shMCT4 constructs (sh1, sh2) with or without supplementation with nucleosides (AUCG). (C) Relative viable cell fractions of HSR-GBM1 shMCT4 Tet-ON cells treated with vehicle (v) or 750nM doxycycline with or without supplementation with all 4 nucleosides (AUCG) or single pyrimidine nucleoside (cytosine, C, or uridine, U). γH2AX immunostaining of HSR-GBM1 (D) and HSR040821 (E) neurospheres that express control or 1 of 2 shMCT4 constructs (sh1, sh2) with or without supplementation with nucleosides (AUCG). (F) γH2AX immunostaining of HSR-GBM1 shMCT4 Tet-ON cells treated with vehicle (v) or 750 nM doxycycline with or without supplementation with either cytidine or uridine. Leflunomide, a DHODH inhibitor, reduces the relative viable cell fraction (G) and induces DNA damage, shown as fold change in γH2AX-positive nuclei (H). Both effects can be readily rescued by exogenous supplementation with uridine (U). Statistics used: one-way ANOVA with Bonferroni correction; * $P < .05$, ** $P < .01$, *** $P < .001$, **** $P < .0001$.

MCT4 Depletion Increases Survival Alone and in Combination With IR

Standard of care ionizing radiation directly affects DNA structure by inducing DNA breaks, particularly, DSBs. The robust induction of DNA damage we documented in hypoxic, MCT4-depleted, neurospheres prompted us to evaluate the potential combinatorial effects of MCT4 depletion with IR. To this end, we established orthotopic xenografts of HSR-GBM1 shMCT4 Tet-ON integrating a constitutive firefly luciferase reporter. Fourteen days after tumor implantation the mice were segregated into the following 4 treatment groups: standard chow (control), radiation (12 Gy), doxycycline (dox), and the combination of MCT4 depletion and radiation (dox+12 Gy). Each group included roughly an equal number of male and female animals with, on average, similar tumor size as determined by bioluminescence imaging (not shown). Also, a small cohort of animals ($n = 4$) per group were included in biological analyses (Figure 6A–C). MCT4 mRNA levels were significantly inhibited by approximately 96% 3 days post-induction with doxycycline (Figure 6A; $*P < .05$ student t test). Similarly, MCT4 protein levels were inhibited in doxycycline-treated mice (Figure 6B, top panel). Importantly, γ H2AX levels were increased, on average, 1.4-fold in doxycycline-treated mice (Figure 6B, and quantified in Figure 6C $*P < .05$ student t test). Collectively, these data show that MCT4 depletion promotes significant DNA damage in vivo. Importantly, the median survival of mice that received a single dose of 12 Gy radiation increased from 47 to 62 days (log-rank $****P < .0001$, Figure 6D, blue triangles). MCT4 depletion alone increased median survival from 47 to 54 days (log-rank $****P < .0001$, Figure 6D, purple triangles), and the median survival of mice receiving doxycycline and radiation increased to 67 days (log-rank $****P < .0001$, Figure 6D, green triangles), underscoring the benefit of a combinatorial approach based on MCT4 depletion and IR. A comparison of median survival between radiation alone and radiation in combination with MCT4 depletion was found also to be highly significant (log-rank $**P < .01$). Of note, 2 mice from the combinatorial treatment group survived for over 120 days without detectable luciferase activity. Microscopic examination of the brains also failed to detect residual tumor mass in these animals suggesting that complete eradication of tumors was achieved.

Discussion

In this study, we observed that the survival and self-renewal of GSCs decreased with MCT4 depletion, a protein we and others have previously shown to be highly overexpressed in GBMs, particularly in hypoxic conditions which are prevalent in GBM. Using our previously described self-renewal assay in methylcellulose⁶ we found a significant decrease in the self-renewal capacity of GBM neurospheres when depleted of MCT4 and that this decrease is maintained for an extended period as the clonogenic challenge is performed for 10 days following recovery in normoxia. Using GSEA of GBM neurospheres cultured in hypoxia, the enrichment of glycolysis and hypoxia genes sets were

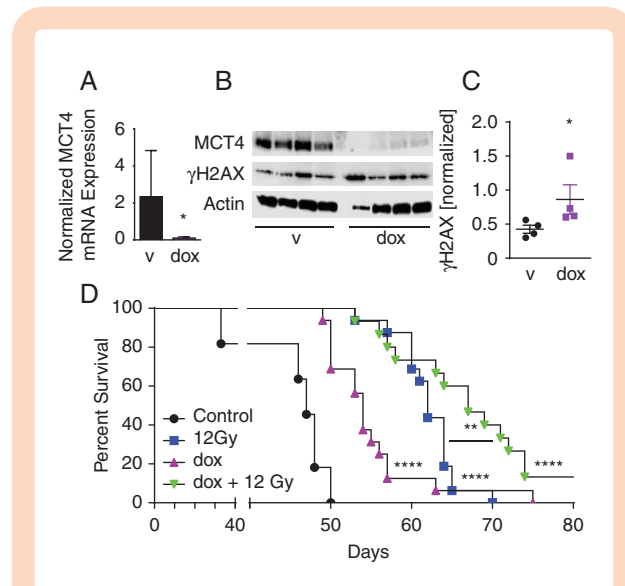


Figure 6. MCT4 depletion inhibits tumor progression alone and in combination with radiation. Intracranial xenografts established with HSR-GBM1 shMCT4 Tet-ON cells integrating a constitutive firefly luciferase reporter. (A and B) qPCR and Western blot analyses for MCT4 mRNA and protein levels ($n = 4$), respectively, performed 3 days after doxycycline (dox) supplementation. (D) Kaplan–Meier survival analysis for 4 treatment groups: standard chow (control), radiation (12 Gy), MCT4 knockdown (dox), and the combination of MCT4 knockdown and radiation (dox + 12 Gy). Statistics used: single-sided t test (A and C; $*P < .05$), log-rank test for survival experiments (D; $**P < .01$, $****P < .0001$).

confirmed. Strikingly, these hypoxia-associated gene signatures were replaced by the oxidative phosphorylation and DNA repair signatures in hypoxic, MCT4-depleted, neurospheres. Also, we documented a considerable reduction in 3-phosphoglycerate phosphate (G3P) and DHAP with a concomitant increase in fructose-1,6 biphosphate, indicating a potential block in aldolase activity. While the regulation of fructose 1,6-bisphosphate aldolase is still not well understood, it has been reported that the activity of one of its isoforms, ALDOC, may be regulated at the transcription level or posttranslational, by oxidation.²⁷ Consistent with this finding, we documented greater than 40% reduction in the expression of ALDOC in hypoxic, MCT4-depleted, neurospheres (Supplementary Figure S4A), suggesting that reduced ALDOC expression may be partially responsible for the accumulation of fructose-1,6 biphosphate and reduction in the immediately downstream glycolytic intermediates produced by aldolase. Also, we found that phosphoenolpyruvate carboxykinase 2 (PCK2), which encodes the mitochondrial form of PCK, was downregulated over 4-fold in MCT4-depleted, hypoxic GBM neurospheres (Supplementary Figure S4B). Given it is the rate-limiting enzyme in gluconeogenesis, converting oxaloacetate to phosphoenolpyruvate, this suggested that gluconeogenesis may also be inhibited by MCT4 depletion. Finally, we found that mitochondrial membrane potential is increased in neurospheres that are depleted of MCT4 and cellular ATP levels were modestly increased. Taken together, these results strongly suggest that MCT4 depletion,

in hypoxia, promotes an inappropriate metabolic switch from glycolysis to oxidative phosphorylation. These data also confirm that MCT4 is critical for maintaining hypoxia-induced glycolysis while inhibiting oxidative phosphorylation under conditions of reduced oxygen.

Our combined transcriptomic and metabolomics approach also identified MCT4 as a critical regulator of de novo nucleotide metabolism in GBM. We documented a significant reduction in the levels of several pyrimidine nucleotides and an increase in DNA damage following MCT4 depletion. Furthermore, supplementation of hypoxic, MCT4-depleted, neurospheres with nucleosides mostly blocked the detrimental effects of MCT4 loss. Given the known relation between nucleotide pools and DNA damage,²⁴ these results suggest that low nucleotide availability is a leading cause for increased DNA damage and concomitant loss of GSC survival following MCT4 inhibition. The question remains, how does MCT4 depletion result in decreased pyrimidine levels? The pyrimidine metabolic pathway (KEGG) includes 57 genes of which 15 were downregulated in MCT4-depleted neurospheres cultured in hypoxia. Two of these genes, DHODH and CAD, are reduced, on average 35%. This provides a potential explanation as to why pyrimidine levels are reduced and to why supplementation with exogenous nucleosides can rescue the defects conferred by MCT4 depletion. A model illustrating the MCT4 role in de novo pyrimidine biosynthesis is shown in Supplementary [Figure S5](#).

Finally, we show that conditional depletion of MCT4 significantly prolongs the survival of animal subjects with established orthotopic GSC-derived xenografts. It is important to note that the analysis of tumor tissues at the time the animals were sacrificed indicated that the tumors all expressed the MCT4 protein at comparable levels (not shown). These results are consistent with our previous report¹⁵ and underscore the absolute requirement for MCT4 in tumor progression. We do acknowledge that while statistically significant, the combination of MCT4 knock-down and radiation showed a modest increase over radiation alone. We suggest that this result is primarily due to the strong effect of the gamma knife radiotherapy. Nevertheless, given that most standard therapies ultimately lead to increased tumor hypoxia and that hypoxia itself can promote a stem cell phenotype and therapeutic resistance in GBM, our demonstration that a combination of MCT4 depletion and ionizing radiation further prolongs survival is significant and provides a strong rationale for testing this combinatorial approach in clinical trials.

Taken together, our studies show that MCT4 plays critical roles in the metabolic adaptation of GSCs to tumor-relevant hypoxic conditions and in maintaining adequate nucleotide pools necessary for the proliferation and survival of GBM cells. Therapies that reduce MCT4 levels are, therefore, a promising new therapeutic approach especially in combination with standard of care radiation therapies.

Supplementary Data

Supplementary data are available at *Neuro-Oncology* online.

Keywords

glioma stem cells | hypoxia | MCT4 | pyrimidine | radiation

Funding

This research was supported by the National Institutes of Health (R01 CA187780 and National Cancer Institute).

Conflict of Interest: None of the authors has a material conflict of interest to disclose.

Authors' Contributions: R.S., D.V.M, X.Y., S.M.W., and N.A. designed and/or performed experiments. J.S., R.V., and A.S. performed experiments. E.B., R.S., H.M.A., and G.F.W. interpreted data. E.B. and R.S. drafted the manuscript. H.M.A., G.F.W., and N.A. assisted in revising the manuscript.

Acknowledgments

We would like to thank Maureen Kachman, PhD and Charles Burant, MD, PhD from the Metabolomics Core at Michigan School of Medicine (Ann Arbor, MI) for performing the metabolomics assays and analysis.

References

1. Stupp R, Mason WP, van den Bent MJ, et al.; European Organisation for Research and Treatment of Cancer Brain Tumor and Radiotherapy Groups; National Cancer Institute of Canada Clinical Trials Group. Radiotherapy plus concomitant and adjuvant temozolomide for glioblastoma. *N Engl J Med*. 2005;352(10):987–996.
2. Huse JT, Holland EC. Targeting brain cancer: advances in the molecular pathology of malignant glioma and medulloblastoma. *Nat Rev Cancer*. 2010;10(5):319–331.
3. Galli R, Binda E, Orfanelli U, et al. Isolation and characterization of tumorigenic, stem-like neural precursors from human glioblastoma. *Cancer Res*. 2004;64(19):7011–7021.
4. Zhou Y, Zhou Y, Shingu T, et al. Metabolic alterations in highly tumorigenic glioblastoma cells: preference for hypoxia and high dependency on glycolysis. *J Biol Chem*. 2011;286(37):32843–32853.
5. Heddlestone JM, Li Z, McLendon RE, Hjelmeland AB, Rich JN. The hypoxic microenvironment maintains glioblastoma stem cells and promotes reprogramming towards a cancer stem cell phenotype. *Cell Cycle*. 2009;8(20):3274–3284.
6. Bar EE, Lin A, Mahairaki V, Matsui W, Eberhart CG. Hypoxia increases the expression of stem-cell markers and promotes clonogenicity in glioblastoma neurospheres. *Am J Pathol*. 2010;177(3):1491–1502.

7. Pistollato F, Chen HL, Rood BR, et al. Hypoxia and HIF1alpha repress the differentiative effects of BMPs in high-grade glioma. *Stem Cells*. 2009;27(1):7–17.
8. Li Z, Bao S, Wu Q, et al. Hypoxia-inducible factors regulate tumorigenic capacity of glioma stem cells. *Cancer Cell*. 2009;15(6):501–513.
9. Seidel S, Garvalov BK, Wirta V, et al. A hypoxic niche regulates glioblastoma stem cells through hypoxia inducible factor 2 alpha. *Brain*. 2010;133(Pt 4):983–995.
10. Soeda A, Park M, Lee D, et al. Hypoxia promotes expansion of the CD133-positive glioma stem cells through activation of HIF-1alpha. *Oncogene*. 2009;28(45):3949–3959.
11. Bar EE. Glioblastoma, cancer stem cells and hypoxia. *Brain Pathol*. 2011;21(2):119–129.
12. Hedderston JM, Li Z, Lathia JD, Bao S, Hjelmeland AB, Rich JN. Hypoxia inducible factors in cancer stem cells. *Br J Cancer*. 2010;102(5):789–795.
13. Bartkova J, Hamerlik P, Stockhausen MT, et al. Replication stress and oxidative damage contribute to aberrant constitutive activation of DNA damage signalling in human gliomas. *Oncogene*. 2010;29(36):5095–5102.
14. Carruthers RD, Ahmed SU, Ramachandran S, et al. Replication stress drives constitutive activation of the DNA damage response and radioresistance in glioblastoma stem-like cells. *Cancer Res*. 2018;78(17):5060–5071.
15. Lim KS, Lim KJ, Price AC, Orr BA, Eberhart CG, Bar EE. Inhibition of monocarboxylate transporter-4 depletes stem-like glioblastoma cells and inhibits HIF transcriptional response in a lactate-independent manner. *Oncogene*. 2014;33(35):4433–4441.
16. Subramanian A, Tamayo P, Mootha VK, et al. Gene set enrichment analysis: a knowledge-based approach for interpreting genome-wide expression profiles. *Proc Natl Acad Sci U S A*. 2005;102(43):15545–15550.
17. Singh NP, McCoy MT, Tice RR, Schneider EL. A simple technique for quantitation of low levels of DNA damage in individual cells. *Exp Cell Res*. 1988;175(1):184–191.
18. Bar EE, Chaudhry A, Lin A, et al. Cyclopamine-mediated hedgehog pathway inhibition depletes stem-like cancer cells in glioblastoma. *Stem Cells*. 2007;25(10):2524–2533.
19. Awan MJ, Dorth J, Mani A, et al. Development and validation of a small animal immobilizer and positioning system for the study of delivery of intracranial and extracranial radiotherapy using the gamma knife system. *Technol Cancer Res Treat*. 2017;16(2):203–210.
20. Wei W, Shi Q, Remacle F, et al. Hypoxia induces a phase transition within a kinase signaling network in cancer cells. *Proc Natl Acad Sci U S A*. 2013;110(15):E1352–E1360.
21. Peñaranda Fajardo NM, Meijer C, Kruyt FA. The endoplasmic reticulum stress/unfolded protein response in gliomagenesis, tumor progression and as a therapeutic target in glioblastoma. *Biochem Pharmacol*. 2016;118:1–8.
22. Voss DM, Spina R, Carter DL, Lim KS, Jeffery CJ, Bar EE. Disruption of the monocarboxylate transporter-4-basigin interaction inhibits the hypoxic response, proliferation, and tumor progression. *Sci Rep*. 2017;7(1):4292.
23. Birsoy K, Wang T, Chen WW, Freinkman E, Abu-Remaileh M, Sabatini DM. An essential role of the mitochondrial electron transport chain in cell proliferation is to enable aspartate synthesis. *Cell*. 2015;162(3):540–551.
24. Juvekar A, Hu H, Yadegarynia S, et al. Phosphoinositide 3-kinase inhibitors induce DNA damage through nucleoside depletion. *Proc Natl Acad Sci U S A*. 2016;113(30):E4338–E4347.
25. Tice RR, Agurell E, Anderson D, et al. Single cell gel/comet assay: guidelines for in vitro and in vivo genetic toxicology testing. *Environ Mol Mutagen*. 2000;35(3):206–221.
26. Nandhakumar S, Parasuraman S, Shanmugam MM, Rao KR, Chand P, Bhat BV. Evaluation of DNA damage using single-cell gel electrophoresis (comet assay). *J Pharmacol Pharmacother*. 2011;2(2):107–111.
27. Sultana R, Perluigi M, Newman SF, et al. Redox proteomic analysis of carbonylated brain proteins in mild cognitive impairment and early Alzheimer's disease. *Antioxid Redox Signal*. 2010;12(3):327–336.